


RESEARCH ARTICLE

Open Access



GMP-compliant automated radiosynthesis of [¹⁸F] SynVesT-1 for PET imaging of synaptic vesicle glycoprotein 2 A (SV2A)

Lijuan Chen¹ , Xiaochen Li¹, Yao Ge¹, Huiqiang Li¹, Ruili Li², Xiaosheng Song³, Jianfei Liang⁴, Weifeng Zhang¹, Xiaona Li¹, Xiaoqi Wang², Yunjuan Wang^{3,5}, Yaping Wu¹, Yan Bai¹ and Meiyun Wang^{1,3*}

*Correspondence:

Meiyun Wang

mywang@zzu.edu.cn

¹Department of Medical Imaging, Henan Provincial People's Hospital & the People's Hospital of Zhengzhou University, Zhengzhou 450003, China

²School of Clinical Medicine, Henan University, Kaifeng 475004, China

³Institute of Biomedicine, Henan Academy of Sciences, Zhengzhou 450046, China

⁴Beijing PET CO., LTD,

Beijing 100093, China

⁵School of life sciences, Henan University, Kaifeng 475004, China

Abstract

Background A novel positron emission tomography (PET) imaging tracer, [¹⁸F] SynVesT-1, targeting synaptic vesicle glycoprotein 2 (SV2A), has been developed to meet clinical demand. Utilizing the Trasis AllinOne-36 (AIO) module, we've automated synthesis to Good Manufacturing Practice (GMP) standards, ensuring sterile, pyrogen-free production. The fully GMP-compliant robust synthesis of [¹⁸F] SynVesT-1 boosting reliability and introducing a significant degree of simplicity and its comprehensive validation for routine human use.

Results [¹⁸F] SynVesT-1 was synthesized by small modifications to the original [¹⁸F] SynVesT-1 synthesis protocol to better fit AIO module using an in-house designed cassette and sequence. With a relatively small precursor load of 5 mg, [¹⁸F] SynVesT-1 was obtained with consistently high radiochemical yields (RCY) of 20.6 ± 1.2% (the decay-corrected RCY, n = 3) at end of synthesis. Each of the final formulated batches demonstrated radiochemical purity (RCP) and enantiomeric purity surpassing 99%. The entire synthesis process was completed within a timeframe of 80 min (75 ± 3.1 min, n = 3), saves 11 min compared to reported GMP automated synthesis procedures. The in-human PET imaging of total body PET/CT and time-of-flight (TOF) PET/MR showed that [¹⁸F] SynVesT-1 is an excellent tracer for SV2A. It is advantageous for decentralized promotion and application in multi-center studies.

Conclusion The use of AIO synthesizer maintains high production yields and increases reliability, reduces production time and allows rapid training of production staff. Besides, the as-prepared [¹⁸F] SynVesT-1 displays excellent in vivo binding properties in humans and holds great potential for the imaging and quantification of synaptic density in vivo.

Keywords [¹⁸F] SynVesT-1, SV2A, PET, Radiochemistry, GMP, Trasis allinone

Background

Synaptic vesicle glycoprotein 2 (SV2A) is the most widely distributed subtype of synaptic vesicle transmembrane protein, which existing in almost all types of neurons, such as in the cerebral cortex, and closely related to the release of neurotransmitters, endocrine

exocytosis, and the maintenance of synaptic vesicle homeostasis. The expression of SV2A is associated with various neuro-psychiatric disorders (Portela-Gomes et al. 2000; Wiedenmann et al. 1986). Moreover, SV2A is also expressed in neuroblastoma (Georgantzi et al. 2019), the pancreas, anterior pituitary lobe, and adrenal medulla where the relative incidence of immunoreactive cells is higher compared to syn immunoreactive cells. It has been reported that SV2A can be used for the pathological assessment of neuroendocrine differentiation (NED) in neuroendocrine tumors (NETs) (Guan et al. 2021; Jakobsen et al. 2002).

Thus, in vivo visualization and quantitative analysis of synaptic density offer extensive clinical applications in the diagnosis, treatment monitoring, and mechanistic research of neurological and psychiatric disorders as well as tumors like NED in NETs (Cai et al. 2019). Up to now, Positron emission tomography (PET) imaging of SV2A has a tremendous potential to be utilized as an early-stage biomarker for Alzheimer's disease (AD) (Mecca et al. 2020) (Mecca et al. 2022), Parkinson's disease (PD) (Delva et al. 2020) (Martin et al. 2023), epilepsy (Tang et al. 2022), autism (Bourgeron 2015), stroke (Michiels et al. 2022, 2023), traumatic brain injury (Jamjoom et al. 2021) and Spinocerebellar Ataxia Type 3 (Chen et al. 2023), as well as psychiatric disorders such as schizophrenia and depression in human subjects (Holmes et al. 2019), including [^{11}C]UCB-J (Mecca et al. 2022), [^{11}C]UCB-A (Estrada et al. 2016), [^{18}F] UCB-H (Bastin et al. 2020), [^{18}F] SynVesT-1 (Li et al. 2021), and [^{18}F] SynVesT-2 (Cai et al. 2019). Among them, the fluorine-18-labeled radioligand [^{18}F] SynVesT-1 (also known as [^{18}F] SDM-8 or [^{18}F] MNI-1126), developed by the Yale PET Center, has shown the most favorable in vivo characteristics including high brain uptake, fast and reversible binding kinetics, SV2A specificity, high specific binding signals, and excellent reproducibility in the measurement of quantitative kinetic parameters (Li et al. 2019).

In order to conduct a broader and more in-depth investigation into clinical diseases related to SV2A expression, developing a safe and stable multi-dose [^{18}F] SynVesT-1 radioactive imaging agent production process is of great significance. Kenneth Dahl and the co-workers had fully automated radiosynthesis of [^{18}F] SynVesT-1, which performed according to good manufacturing procedure (GMP) using a commercially available module (TracerMaker, ScanSys Laboratorieteknik ApS, Copenhagen, Denmark) with minor changes, and result a high-yield, acceptance criteria and quality control (Dahl et al. 2022). In comparison to similar modules, Trasis AllinOne (AIO) is described as being versatile and capable of handling complex chemistry. This product not only can synthesize [^{18}F] labeled drugs but also [^{68}Ga] and [^{177}Lu] labeled drugs. The instrument can be broken down to the chemistry module, purification module and reformulation module. Disposable cassettes, reagents and components are used to ease the burden on cleaning. Successful production with high yield and high specific activity to the following compound, such as [^{18}F] labeled [^{18}F] FDG (Barnes et al. 2022), [^{18}F] F-DPA-714 (Cybulska et al. 2021a), [^{18}F] FAPI-74 (Cybulska et al. 2021b), [^{18}F] FES (Otabashi et al. 2017a), [^{18}F] FET (Otabashi et al. 2017b), and [^{18}F] FMZ (Gendron et al. 2022), and [^{68}Ga] labeled (Da Pieve et al. 2022) has been reported. These radiotracers were developed many years ago and have been used on either an intermediate to widespread basis in PET imaging studies. Currently, in our PET center, we developed the full-automated synthesis module can produce more than 10 different drugs ([^{18}F] DOPA, [^{18}F] TSPO, [^{68}Ga] DOTATATE, et al.) for research use.

Here, we developed a full-automated and commercially-available synthesis on AIO module, which was developed as a universal GMP-compliant synthesis module for radiolabeling of radiotracers with short half-life radionuclides. Besides, we evaluated the PET imaging of SV2A in healthy volunteer by analysis of the GMP level [^{18}F] SynVesT-1 imaging data.

Materials and methods

Materials

Reagents and cartridges

All chemicals and reagents were obtained from commercial vendors and used as received without further purification, except for the precursor $\text{Me}_3\text{Sn-SDM-8}$ and standard sample [^{19}F] SynVesT-1, which provided by prof. Fang Xie from Huashan Hospital and Prof. Huang from PET center of Yale University, the synthesis route and structure determination of the precursors were based on the methods in the article by Yiyun Huang (Li et al. 2019). Details of the reagents and consumables required for preparation are presented in Table 1.

Human subjects

The study was approved by the Research Ethics Committee of Henan Provincial people's hospital and written informed consents were obtained from the subjects. Both subjects were screened with a physical exam, medical history, routine laboratory studies, and electrocardiography to assess for eligibility.

Methods and GMP radiosynthesis

Production of [^{18}F] fluoride

[^{18}F] Fluoride ($^{18}\text{F} \text{F}^-$) was produced via the standard $^{18}\text{O}(\text{p}, \text{n})^{18}\text{F}$ nuclear reaction, by irradiating cyclotron target containing [^{18}O]water with a proton beam (9.4 MeV) of 40 μA for 50 min (Mini trace PET cyclotron, GE, Uppsala, Sweden). The typical amount of [^{18}F] F^- produced was approximately 29.6 GBq (800 mCi).

Cassette placements

Following a series of machine tests, upon receiving the command from the software, the cassette, which includes the quaternary methyl ammonium (QMA) cartridge, tC18 cartridge, and Alumina N cartridges, is appropriately positioned within the machine. Subsequently, a comprehensive self-check of both the equipment and the cassette is conducted before initiating the high-performance liquid chromatography (HPLC) priming process.

HPLC priming

In parallel, the HPLC pump is initiated to achieve column equilibration in a mixture of 25% acetonitrile (MeCN) in buffer (0.1 M ammonium formate solution with 0.5% ethanoic acid AcOH, pH 4.2) at a flowrate of 5.0 ml/min maintained for 20 min. We utilize a single-channel mixed mobile phase that has been filtered, homogenized, and thoroughly degassed through ultrasonication to ensure stable pressure, avoiding the instability issues associated with dual-channel online mixing. After a 20-minute equilibration, the

Table 1 List of chemicals in the reagent and cartridges required to assemble the cassette for one [¹⁸F] SynVesT-1 production on the Trasis AIO-36 module

Position	Item	Composition	Qty	Container	Manufacturer	Storage
5	Sep-Pak Accel Plus QMA Carbonate Light Cartridge (46 mg sorbent/cartridge)	QMA Carbonate	1	NA	Waters	RT
11 (Site E)	Sep-Pak Plus Alumina N Cartridges-280 mg	Al ₂ O ₃	1	NA	Waters	RT
13	Sep-Pak tC18 Plus Short Cartridge, 400 mg Sorbent per Cartridge	tC18	1	NA	Waters	RT
2 (Site A)	Acetonitrile	Anhydrous acetonitrile	2 mL	4 mL clear glass vial	Sigma-Aldrich	RT
3 (Site B)	QMA Eluent	K ₂ CO ₃ (1 mg/ml) of distilled water	50 µL	3 mL BD syringe	Sigma-Aldrich	Fridge
		KOTf (10 mg/ml) of distilled water	450 µL		Aladdin	
		Acetonitrile	500 µL		Macklin	
8 (Site C)	Precursor	Me ₃ Sn-SDM-8	5 mg	4 mL amber glass vial	Provided by Huashan hospital	Fridge
		Tetrakis(pyridine) copper (II) triflate	35 mg		Bidepharm	
		Anhydrous N, N-dimethylacetamide	1 mL		Aladdin	
10 (Site D)	Dilution	Aqueous buffer: 25% CH ₃ CN and 75% 0.1 M ammonium formate solution with 0.5% acetic acid (AcOH) (pH 4.2)	10 mL	20 mL clear glass vial	HPLC Solvent A	Fridge
14 (Site F)	Ethanol	Ethanol absolute ChP	10 mL	20 mL clear glass vial	Macklin	RT
15 (Site G)	Empty vial		50 mL	50 mL	---	RT
17 (Site H)	Bag of sterile injection water	Sterile injection water	500 mL			RT
HPLC Solvent A	Aqueous buffer: 25% CH ₃ CN and 75% 0.1 M ammonium formate solution with 0.5% AcOH (pH 4.2)	Ammonium formate	3.15 g	500 mL	Sigma-Aldrich	RT
		acetic acid	2.5 mL		Sigma-Aldrich	RT
		CH ₃ CN	125 mL		Sigma-Aldrich	RT
		H ₂ O	500 mL		DI water	RT
HPLC Solvent B	Ethanol	Ethanol anhydrous, Ph.	500 mL	300 mL	Macklin	RT
HPLC Solvent C	10% (v/v) ethanol in H ₂ O	Ethanol anhydrous, Ph.	1000 mL		Macklin	RT

flow rate will be set to 3 ml/min until loading the sample, at which point the injection triggers the flow rate to return to 5 ml/min.

Preliminary steps and reagent placements

Prepare the reagents according to Table 1 at ambient laboratory conditions. Both the precursor and the tetrakis(pyridine) copper (II) triflate are solubilized manually before starting the procedure to ensure solubilization of the copper reagent. The standard procedure to prepare these vials is given below:

(1) Using a 1 ml sterile hypodermic syringe equipped with a 23G needle (SHANDONG WEIGAO GROUP ME), withdraw 0.5 ml of anhydrous N, N-dimethylacetamide

(DMA, Aladdin, China), dispense 0.50 ml of the solvent into the precursor vial (amber glass, purple crimp), piercing through the center of the septum. (2) Using a new 1 ml syringe equipped with a 23G needle, withdraw 0.50 ml of anhydrous DMA, dispense 0.50 ml of the solvent into the tube with tetrakis(pyridine)copper (II) triflate prepared in advance to obtain the blue, clear solution. (3) Shake the vial and tube vigorously to fully solubilize, and transfer the whole copper catalyst into the precursor vial and mix evenly. Check visually for remaining solid in the vial before placing on the cassette. (4) The QMA carbonate Light cartridge (V5) was pre-activated with ethanol (EtOH, 5 ml), a solution of potassium triflate (KOTf) in de-ionized (DI) water (90 mg/ml, 5 ml), and DI water (5 ml). (5) The Alumina N cartridge (V11) was pre-activated with 20 ml of DI water and 10 ml of air. (6) The tC18 cartridge (V13) is conditioned with 6 ml EtOH (V14) and 10 ml water for injection (V17), using the 20 ml BD Syringe (V9). (7) The reagents are placed on the cassette as shown on Fig. 1, when prompted by the command software.

Radiosynthesis of [^{18}F] SynVesT-1

A schematic diagram of the AIO module used for the synthesis of [^{18}F] SynVesT-1 is shown in Fig. 1. The inhouse developed sequence for [^{18}F] SynVesT-1 includes all key production steps: (1) trap and release of cyclotron produced [^{18}F] F using an ion-exchange cartridge, (2) azeotropic drying of [^{18}F] F $^{-}$, followed by (3) copper mediated [^{18}F] fluorination of the Me $_3$ Sn-SDM-8 precursor compound (Scheme 1), (4) HPLC purification, and (5) formulation of the final product. A more detailed description follows:

- 1) The [^{18}F] fluoride in [^{18}O] water is received from the cyclotron and transferred into the activity reservoir on V6.

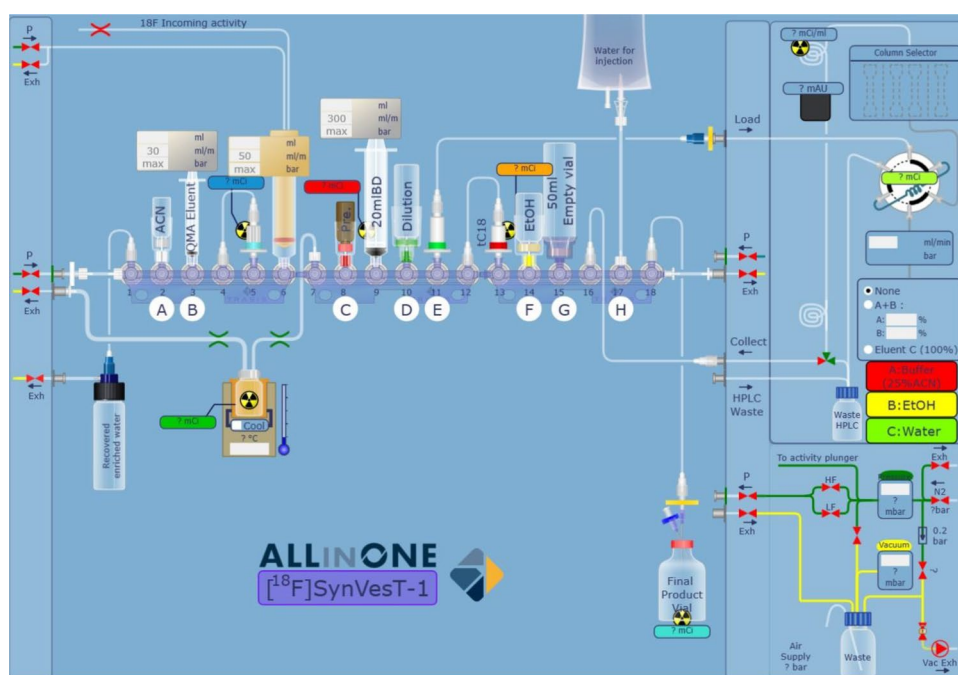
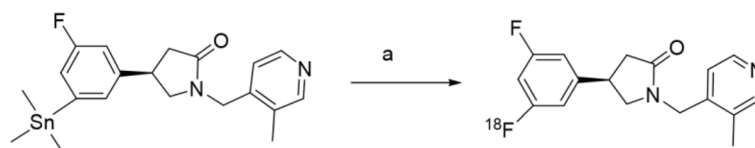


Fig. 1 The cassette layout for radiosynthesis of [^{18}F] SynVesT-1 on a Trasis AIO-36 module allows control through the user software interface



Reagents and conditions: (a) Tetrakis(pyridine)copper (II) triflate, K¹⁸F, DMA, 120 °C, 20 min

Scheme 1 Radiosynthesis of [¹⁸F] SynVesT-1

- 2) The radioactive solution is subsequently transferred through the pre-activated QMA cartridge to separate [¹⁸O] H₂O and effectively trapping the [¹⁸F] fluoride, and the eluate is directed toward the Recovered enriched water collection vial (V6-5-4-1).
- 3) After a brief flush of the QMA and lines, the QMA eluent is withdrawn from the 3 ml BD syringe (V3) and is subsequently passed through the QMA toward the reactor to release the activity (V4-5-7- reactor).
- 4) The [¹⁸F] fluoride is then azeotropically dried under vacuum/nitrogen flow using a gradient of temperature (105 °C) for 4 min.
- 5) In order to thoroughly dry [¹⁸F] fluoride, 1 ml anhydrous acetonitrile was added from V2 to the reactor, dried for 4 min, and repeated once, respectively.
- 6) The reactor is then actively cooled to 90 °C using a flow a compressed air.
- 7) The precursor Me₃Sn-SDM-8 and the tetrakis(pyridine) copper (II) triflate in *N,N*-dimethylacetamide are successively added into the reactor by pressure-transfer.
- 8) The reactor temperature is set to 120 °C, reaction timer is set to 20 min. The reactor is closed in the entire reaction process.
- 9) At the end of the 20 min reaction, the reactor is actively cooled to 50 °C before the reaction mixture is diluted through the 20 ml BD syringe, the quench solution is pre-prepared by withdrawing 4 ml contain 25% MeCN in buffer (0.1 M ammonium formate solution with 0.5% AcOH (pH 4.2) (V10) in the 20 ml BD syringes (V9), suction and mix three times through the syringe.
- 10) The crude reaction mixture (1 ml) and the dilution (4 ml) is load to the HPLC loop circle through the Alumina N cartridge (V11) and a sterile nylon syringe filter at load site to separate of insoluble impurities.
- 11) Additionally, the reactor is subsequently rinsed with another 4 ml of dilution using the 20 ml BD Syringe, repeating the step 10) to thoroughly transfer the potentially remaining crude reaction mixture. Finally, total 9 ml of sample is loaded on the loop circle and ready for injection to HPLC.
- 12) In parallel to the reaction, after the 20 min's HPLC column equilibrate, the HPLC pump is maintain a flow rate of 3 ml/min, and the HPLC mobile phase waste is collected in HPLC waste.
- 13) As the injection loop is turned into the inject position, the acquisition software starts monitoring the Ultraviolet (UV), the radioactivity, flowrate, and the pressure in the HPLC system. And the flowrate switch to 5.0 ml/min, HPLC conditions as follow: 25% MeCN in buffer (0.1 M ammonium formate solution with 0.5% AcOH (pH 4.2) on a XBridge®BEH OBD™ C18 column (5 μm, 130 Å, 10 mm × 250 mm).
- 14) Whilst the semi-preparative purification proceeds, the line (V9-V18) has been rinsed twice with 20ml H₂O, and the flushing waste liquids flows into the waste bottle.

- After that, 10 ml of water for injection (V17) is transferred and added to the vacuumed empty vial of intermediate transfer (V15) by 20 ml BD Syringe.
- 15) After approximately 20 min, the [^{18}F] SynVesT-1 elutes from the column and is collected by switching the collection valve as well as V15-16 to direct the empty vial (V15).
 - 16) The collection is manually begun and manually stopped or stopped automatically after 2.5 min, whichever happens first. And the product is collected in the intermediate transfer vial (V15).
 - 17) Formulating, with the assistance of a 20 ml syringe (V9), another 20 ml of water for injection was added in the vial (V15). After thorough mixing several times with the 20 ml syringe (V9), repeat the process twice by passing the liquid from the intermediate transfer vial (V15) through a tC18 cartridge (V13). This is done to adsorb the product onto the tC18 and concentrate it.
 - 18) The tC18 cartridge (V13) is subsequently washed with 20 ml of water for injection (V17) to wash away ion-type impurities.
 - 19) [^{18}F] SynVesT-1 is released from the tC18 cartridge by injecting 1 ml ethanol (V14-13-12-9) and 4 ml water for injection solution (V17-13-12-9) to final product vial (FPV).
 - 20) The final product is diluted with another 7 ml water for injection (V17) using the 20 ml BD Syringe and flow toward the FPV filtered through a 0.22 μm sterile filter (Vented Millex[®]-GV, MERCK Millipore, Ltd) and reach a final volume of 11 ml.
 - 21) After flushing the delivery line with nitrogen, the final product is ready for dispensing and quality control.
 - 22) Empty all reagent vials, and the cassette is thoroughly washed to reduce the residual radiation to the lowest level achievable. In parallel, the HPLC column is washed successively with water (to remove ammonium formate buffer) and finally stored in ethanol.

Quality control (QC)

All the QC tests were conducted on the formulated product solutions, and the obtained results are in accordance with the standards for injection solutions specified in the Chinese Pharmacopoeia (ChP, 2020), Impurities: ICH Q3C(R8) Guideline for Residual Solvents and ICH Q3C(R2) Guideline for Elemental Impurities. (Table 2)

Final volume

The total solution volume in the ultimate product vial was determined by the weighing of the Final Product Vial (FPV), taking into account the initial tare of the vial. Accurate determination of both volume and activity concentration is imperative to ensure the radio-HPLC detection range and ascertain radiochemical purity.

Appearance

The content of the final product vial was visually assessed behind appropriate shielding. The solution must be clear, colorless, and free of visible particulate matter.

Table 2 Acceptance criteria and quality control results from three productions of [¹⁸F] SynVesT-1 using the AIO-36 module

Test item	Batch 1	Batch 2	Batch3	Acceptance criteria	Method	Reference
Radioactivity per batch	2.96 GBq	6.39 GBq	3.93 GBq	Not specified	Dose calibrator	*NA
Radiochemical yield (%)	13.1%	12.89%	11.82%	Not specified	FPV activity/ QMA activity	*NA
Radiochemical yield (%) decay-corrected	21.79%	20.68%	19.32%	Not specified	Activity meter	*NA
Appearance	Pass	Pass	Pass	Clear, colorless, free from particles	Visual inspection	ChP
pH	6.0	6.0	6.0	4.5–8.0	pH indicator strip	ChP
Molar activity	64.34	98.30	78.6	55.5 GBq/μmol	radio-HPLC	ChP
Product identity	0.427	0.375	0.555	[Rt radiopeak - Rt UV] = 0.2–0.6 min	radio-HPLC	ChP
Radiochemical purity	100%	99.9%	100%	≥ 95%	radio-HPLC	ChP
Enantiomeric purity	100%	100%	100%	≥ 95%	radio-HPLC	ChP
Bacterial endotoxins(EU/ml)	< 0.10	< 0.10	< 0.10	< 15 EU/ml	Dynamic Turbidity Method	ChP
Sterility	Sterility	Sterility	Sterility	Sterility	Membrane Filtration Method	ChP
Residual DMA	n.d.	n.d.	n.d.	≤ 1090 ppm	GC	ICH (Q3C) R8
Residual acetonitrile	n.d.	n.d.	n.d.	≤ 410 ppm	GC	ICH (Q3C) R8
Ethanol content	8.7%	9.2%	9.6%	≤ 10%	GC	Serdons et al. 2008
Residual copper content (μg/l)	429.80	387.52	358.29	300 μg/day for injection	ICP-MS	ICH (Q3C) R2
Residual copper content (μg/Vmax)	4.73	4.26	3.94			

*NA: Not applicable

pH

pH was measured using a pH meter (OHAUS, Starter 2100) calibrated at pH 4.0, 7.0 and 10.0 with correction for the temperature. The results were cross-checked with two pH paper strips of different ranges. According to the Chinese Pharmacopoeia (ChP), the pH range of injection solutions should be 4–9.

Semi-preparative HPLC

The Semi-preparative HPLC separation and analysis as part of tracer production, the crude product solution was purified by the AIO-36 equipped semi-preparative chromatography XBridge®BEH OBD™ C18 column (5 μm, 130 Å, 10 mm × 250 mm). The chromatographic fraction containing the product was collected a mixture of 25% acetonitrile (MeCN) in buffer (0.1 M ammonium formate solution with 0.5% ethanoic acid AcOH, pH 4.2) at a flowrate of 5.0 ml/min.

Analytical HPLC methods

HPLC methods were developed for testing the key quality characteristics: product identity, radiochemical purity (RCP), enantiomeric purity and stability. The key quality characteristics were determined by analytical radio-HPLC using Agilent (1260) System equipped with a quaternary pump (G7111A), manual injector, DAD WR array ultraviolet detector (G7115A), and radio detector (Eckert & Ziegler, B-FC-1000).

Radiochemical purity (RCP) and product identity

Refer to the chromatographic conditions in Sect. 2.3.5, the identity of the radiochemical product [^{18}F] SynVesT-1 was confirmed by coinjection with the non-radioactive analogue [^{19}F] SynVesT-1 authentic standard sample. Product identity, RCP analysis was performed on an analytical Chromolith Performance RP-C18 column (150×4.6 mm, 5 μm ; Luna, USA) by gradient elution (Table 3) at the flow rate of 1 ml/min. And the RCP calculate according to the proportion of the total radioactivity in a sample present as the desired radiolabeled [^{18}F] SynVesT-1. (RCP=[^{18}F] SynVesT-1 radioactivity/total radioactivity*%).

Enantiomeric purity analysis

Enantiomeric purity analysis was performed on a chiral analytical column (LUX[®], Cellulose-1, 250×4.6 mm i.d., 5 μm) with the same HPLC analysis method under the conditions of Sect. 2.3.5.

Residual solvents and ethanol content

Quantification of residual solvents and ethanol content was achieved with quantitative Gas Chromatography (GC). Solvent levels were analyzed using a gas chromatograph (GC, QSP-A-P013, Agilent) equipped with a flame ionization detector (FID), a Quartz elastic capillary column (30 m×0.32 mm×1.8 μm , Agilent DB-624), and an autoinjector.

Residual copper content

Three samples were analyzed with inductively coupled plasma mass spectrometry (ICP-MS, Agilent 7800) to determine the residual copper content. Briefly, the solution must be clear without the presence of precipitates or insoluble materials, and dilute 1 ml of the sample to 10 ml, and directly perform on-machine testing for the concentration of copper. The resulting solution was analyzed by ICP-MS.

Sterility and bacterial endotoxins test

The [^{18}F] SynVesT-1 productions were tested for microbiological contamination by inoculation in fluid thioglycolate (FT) medium and tryptic soy broth (TSB) medium by membrane filtration method according to general Chap. 1101 of the Chinese Pharmacopoeia (2020 Edition, Part IV). The endotoxins test is based on the dynamic turbidity method under general Chap. 1143 (ChP, 2020 Edition, Part IV). The tests and analysis were performed by GUANGDONG DETECTION CENTER OF MICROBIOLOGY (Guangzhou, China).

Table 3 Gradient elution method of UV & Radio dual detectors HPLC

Time (min)	A: 0.1 M ammonium formate solution with 0.5% AcOH (pH 4.2) (%)	B: MeCN (%)
0.00	100	0
2.00	100	0
12.00	70.0	30.0
32.00	45.0	55.0
32.50	10.0	90.0
36.00	10.0	90.0
36.50	100.0	0
40.00	100.0	0

Radiological examination with PET/CT and PET/MR

PET/Computed Tomography (CT) imaging was done on Total-body scanner (uEXPLORER, UNITED IMAGING, CHINA) and time-of-flight (TOF) PET/Magnetic Resonance (MR) (uPMR[®]790, UNITED IMAGING, CHINA) in Henan Provincial People's Hospital, Zhengzhou, Henan Province, PRC. Volunteer was given [¹⁸F] SynVesT-1 at a dose of 388 MBq (5.55 MBq/kg, 70 kg). The delineation of regions of interest was performed by experienced radiologists. Furthermore, these diagnoses are prevalent enough that we can discuss specific scans without jeopardizing the privacy and confidentiality of the individuals involved.

Statistical analysis

All data were statistically analyzed with one-way analysis of variance (ANOVA), and list in the form of mean value \pm standard deviation (SD) values.

Results

The automated radiochemical synthesis and QC results

Final volume, appearance and pH

With a single production batch, starting with 22–50 GBq of [¹⁸F] fluoride, between 2 and 7 GBq of the tracer can be produced. The QC results from three productions of [¹⁸F] SynVesT-1 are outlined in Table 2. The final volume of the prepared product is a 12-milliliter ethanol-water solution. All the final product solutions were clear, colorless, and free of visible particulate matter. All the pH of the final product solutions were 6.0 (Table 2).

Product identity, RCP analysis

Radioactive products require online preparative separation with AIO-36 module platform to exclude radioactive impurities as well as non-radioactive impurities such as unreacted excess precursors. Under the condition, the retention time of [¹⁸F] SynVesT-1 was approximately 19 min (1140 s) (Fig. 2). Besides, product identity, RCP analysis was performed on an analytical Chromolith Performance RP-C18 column (150 \times 4.6 mm, 5 μ m; Luna, USA) by gradient elution (Table 3) at the flow rate of 1 ml/min. Radiochemical purity and identity of [¹⁸F] SynVesT-1 were confirmed by co-injecting the test samples at defined time periods with standard [¹⁹F] SynVesT-1 on an HPLC chromatography system and analyzing the UV and radioactive peak areas which eluted along with standard [¹⁹F] SynVesT-1. The retention time for the [¹⁹F] SynVesT-1 authentic standard sample was observed at 19.798 min, while the labeled product [¹⁸F] SynVesT-1 exhibited a retention time of 20.226 min (Fig. 3), and from the radio signal, the radiochemical purity (RCP) was about 100%. Enantiomeric purity analysis was performed on a chiral analytical column (LUX[®], Cellulose-1, 250 \times 4.6 mm i.d., 5 μ m) with the same HPLC analysis method. Retention time of the [¹⁹F] SynVesT-1 ((R)-SDM-8) reference was 24.702 min, and [¹⁸F] SynVesT-1 eluted at 25.274 min without any other radioactive by-products and non-radioactive species (Fig. 4).

Residual solvents, ethanol content and copper content

In radiopharmaceutical chemical quality control, monitoring and controlling residual solvents, ethanol content, and copper content help ensure the quality, safety, and efficacy

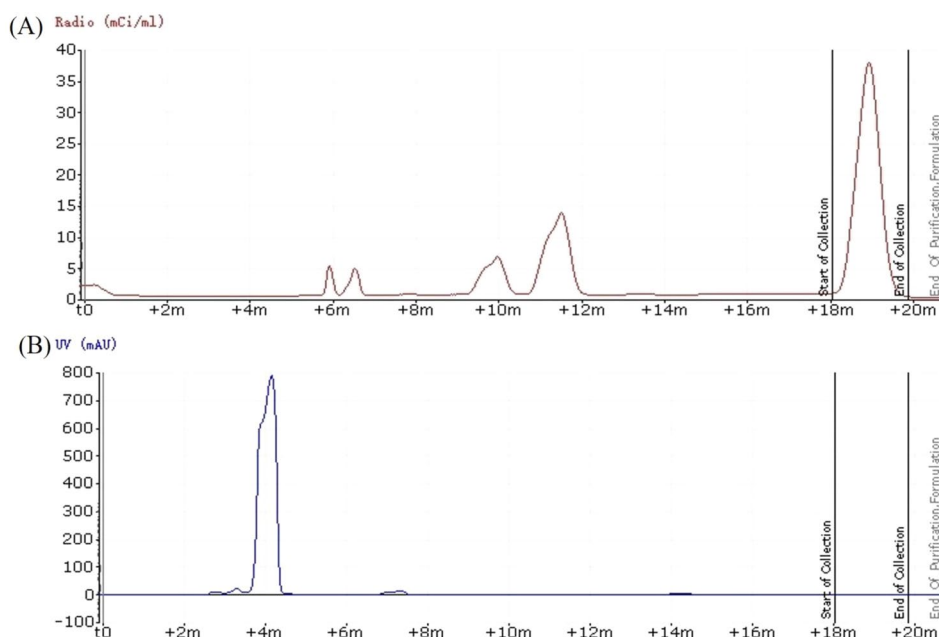


Fig. 2 Typical semi-preparative HPLC purification chromatogram of a [^{18}F] SynVesT-1 production under optimized conditions on the AIO-36 module by Trasis. **(A)** The red chromatogram corresponds to radiation detection, whereas the blue chromatogram **(B)** corresponds to UV detection ($\lambda = 254 \text{ nm}$)

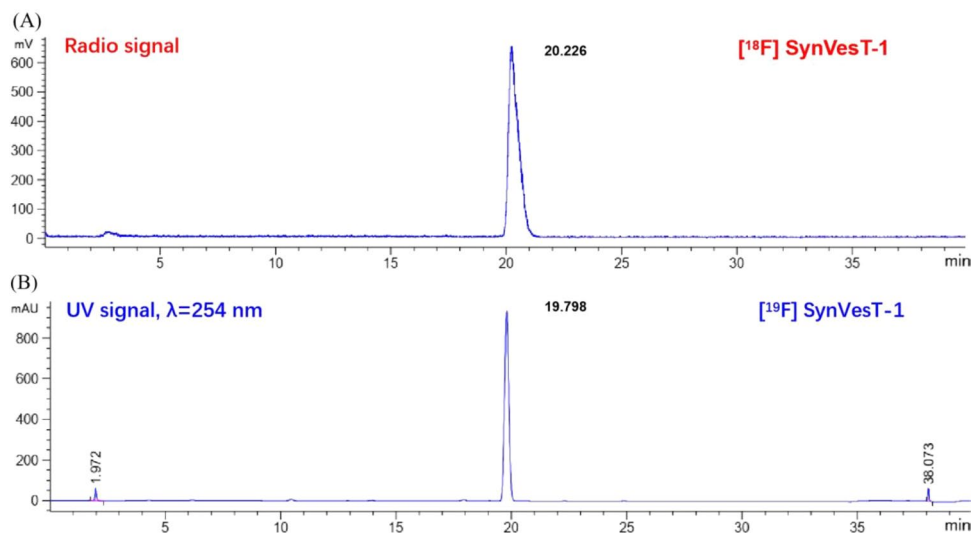


Fig. 3 Typical-Radio HPLC chromatogram ($\lambda = 254 \text{ nm}$) coinfection of [^{18}F] SynVesT-1 production with [^{19}F] SynVesT-1 reference standard ($100 \mu\text{g/ml}$). **(A)** The upper chromatogram corresponds to radiation detection. Whereas the chromatogram **(B)** corresponds to UV detection ($\lambda = 254 \text{ nm}$)

of the drugs, thereby safeguarding patient interests. The limited concentration of ethanol is no more than 10% (V/V) ($\text{EtOH} \leq 10\%$) when added as an excipient or solvent in radiopharmaceutical injections (Serdons et al. 2008), and according to the ICH(Q3C) the limitation are $410 \mu\text{g/l}$ of acetonitrile (MeCN) and 1090 ppm of DMA (Table 2). The production of both acetonitrile and DMA content cannot be detected (n.d), and the ethanol content of all three batches of samples does not exceed 10%. The average content of residual copper is $391.87 \pm 35.95 \mu\text{g/l}$ ($4.31 \pm 0.39 \mu\text{g/Vmax}$), this result complies with the injection limit requirements at the ICH(Q3C) limit Permitted Daily Exposures (PDE)

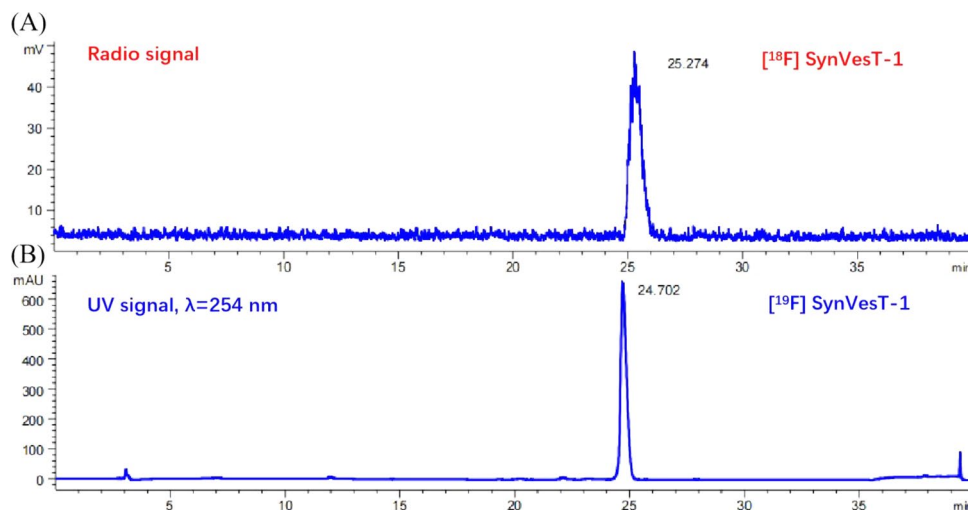


Fig. 4 Analytical chiral high-performance liquid chromatography (HPLC) chromatogram coinfection of [¹⁸F] SynVesT-1 production with [¹⁹F] SynVesT-1 reference standard (100 µg/ml). **(A)** The upper chromatogram corresponds to radio signal detection. Whereas the chromatogram **(B)** corresponds to UV detection (λ = 254 nm)

for copper elemental impurities 300 µg/day/person for injection, the injection volume per person is less than 2 ml based on the activity concentration during the PET imaging. (Table 2)

Sterility and bacterial endotoxins test

Based on traceability testing for sterility, the results indicated that the colony count of the positive control in thioglycollate fluid medium was 71 CFU/ml. The three different batches of products tested exhibited sterile growth after 14 days of culture in FT and TSB medium. Concurrently, a negative control was included in the test, confirming sterile growth. These findings confirm the sterility of the [¹⁸F] SynVesT-1 products.

Total body PET/CT imaging analysis

The 90 min dynamic data were reconstructed at 10 min intervals and the resulting groups were named T0-10, T10-20, T20-30, T30-40, T40-50, T50-60, T60-70, T70-80 and T80-90. [¹⁸F] SynVesT-1 PET maximum intensity projection (MIP) images acquired in different time windows show the biodistribution of the radiotracer over time (Fig. 5). [¹⁸F] SynVesT-1 is rapidly distributed throughout the body following intravenous administration, particularly in hyperperfused organs such as the brain, liver, kidney and bladder. Subsequently, the tracer shows rapid clearance with a relatively short plasma half-life.

PET/MR brain imaging analysis

Healthy volunteers [¹⁸F] SynVesT-1 showed high uptake and heterogeneous distribution in the human brain. High levels of radioactivity were observed in all grey matter regions and low uptake in white matter regions (Figs. 5 and 6). The highest uptake in volunteer brain tissue was found in the bilateral frontal cortex and putamen, and the lowest in the centrum semiovale. Uptake was significantly lower in the centrum semiovale of the hemisphere of the volunteer brain than in any of the grey matter regions tested. [¹⁸F] SynVesT-1 showed good kinetics in all grey matter regions, with peak uptake in all brain

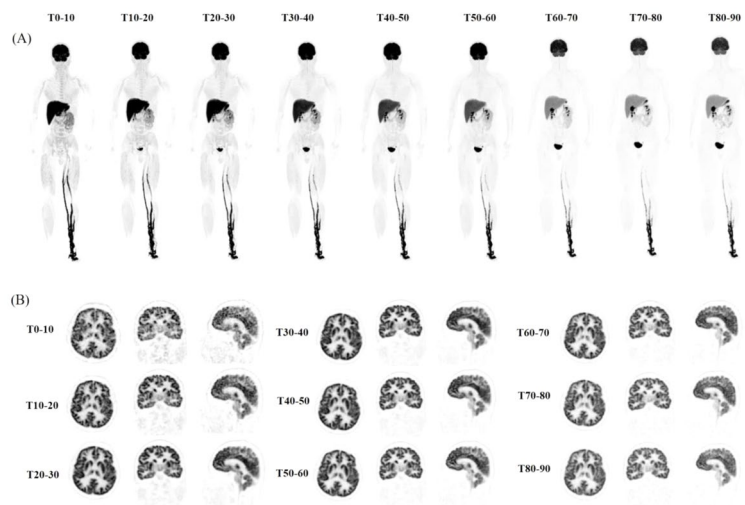


Fig. 5 Total body PET images of representative [^{18}F] SynVesT-1 scan with PET/CT from 0 to 90 min after injection and image reconstruction of whole body (A) and brain (B) occurs every 10 min

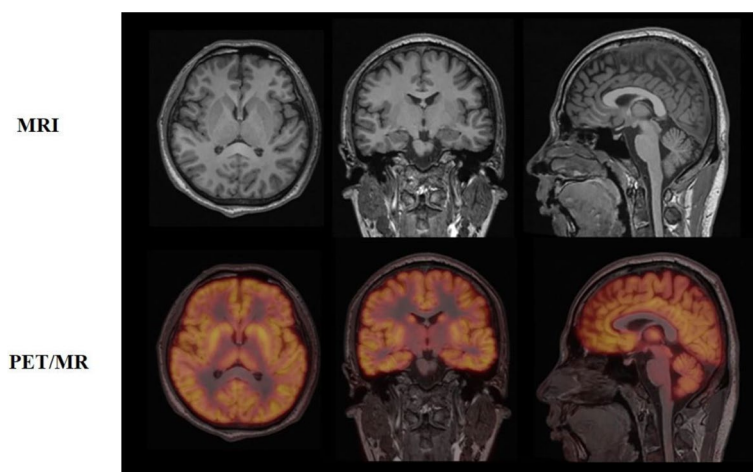


Fig. 6 [^{18}F] SynVesT-1 PET/MR imaging of brain

regions within approximately 30 min after injection, followed by a steady decrease in regional radioactivity over time.

Discussion

Only small modifications to the original [^{18}F] SynVesT-1 synthesis protocol presented by Li et al. (Li et al. 2019) was made to better fit AIO-36 module by Trasis with the corresponding organotin precursor. Firstly, tetrakis(pyridine)copper (II) triflate as the catalyst which serves to coordinate both the aryl and fluoride ligands and promote their coupling, and copper (II) triflate can provide activated fluorination reagent to promote the reaction. Compared to the use of pyridine and a solution of copper (II) triflate as catalysts in the literature (Li et al. 2019), tetrakis(pyridine)copper (II) triflate is a well-defined complex, as one of the commonly used catalysts for fluorination reactions, making it easier to control reaction conditions and improve reproducibility, potentially yielding fewer side reactions and enhancing reaction reproducibility, thus suitable for clinical applications in different model. However, considering the dosage and solubility

of copper salts, the fluorination reaction produces a crude solution that is both turbid and deeply saturated in blue color, thorough purification is required before injection into HPLC. Alumina N plus light cartridge plays a crucial role in this step, after extensive water pre-activation, it can obstruct most insoluble precipitates. To further safeguard the operation of the HPLC system, a sterile needle filter with hydrophobic membrane filter is required to connect the HPLC loop injection line and the alumina N plus light cartridge before loading the liquid, preventing column pressure elevation or clogging caused by insufficiently filtered precipitates or Al_2O_3 column packing material.

Additional modification was the reaction temperature, it was known that not to cause racemization of the product when the reaction carried out at 110 °C. The experimental conditions were finally verified that there is no racemization under the reaction conditions of 120 °C and 20 min according to the enantiomeric purity analysis results (Fig. 4). Because of the inherent half-life properties of radiopharmaceuticals, synthesis and purification time are critical for promotion and application. Our work took an average of 75 min including purification and formulation, 1/3 less than the earliest reported time of 120 min (Li et al. 2019), and 11 min less than the latest automated synthesis procedure (Dahl et al. 2022). With the reaction parameters optimized, our final goal was to conduct 3 process validation batches to qualify the radiosynthesis for clinical research production. In our survey, we are attempting to use ethanol instead of acetonitrile in the mobile phase, that is, we used 25% ethanol in buffer (0.1 M ammonium formate solution with 0.5% AcOH (pH 4.2) as the mobile phase in the process exploration (only one batch). Surprisingly, after analysis and purification on semi-preparative column the peak of the production did not change, but the retention time was delayed by 3 min. From the perspective of solvent safety, it is also possible to minimize the use of acetonitrile Class 2 solvent.

All of the cartridges including the cassette, vial, syringe, cartridge are sterile, as well as the reagents like ethanol, sterile injection water. The final product collected and flow toward the final product vial were filtered through a sterile Millex® PVDF vented syringe filter membrane, and a Millex®-GV sterile air filter membrane was also be used to balance the pressure inside and outside the product container. All the above operations ensure that the product is sterile and free of pyrogens. The radiosynthesis procedure reported here is novel with respect to the reagents, temperatures, and times needed to produce the radiopharmaceutical on a very different automated radiosynthesizer.

SV2A is widely distributed in the nervous system, in virtually all neurons. (Portela-Gomes et al. 2000), including in the brain and the spinal cord (Samantha Rossano et al. 2022). Given the limitations and the limited resolution of the traditional “wholebody” PET/CT imaging compared with the 194-cm-long PET/CT system (uEXPLORER, UNITED IMAGING) (Huang et al. 2022), the as-prepared [^{18}F] SynVesT-1 meets the requirements for human injection and conduct whole-body in vivo imaging scans to assess the distribution of synaptic density in various locations throughout the body. Following intravenous administration, [^{18}F] SynVesT-1 quickly disperses throughout the body, with notable accumulation in highly perfused organs such as the brain, liver, kidneys, and bladder. To our knowledge, this is the first human whole-body imaging of SV2A, laying the foundation for exploring its systemic applications in patients of synaptic loss-related diseases. Moreover, it has been reported that SV2A can be used for

pathological assessment of NED in NETs (Guan et al. 2021), whole-body imaging of SV2A contributes to the diagnosis and localization of such tumors.

Conclusion

In summary, the protocol consistently delivers a sterile and pyrogen-free product adhering to good manufacturing practice (GMP) standards—specifically, [^{18}F] SynVesT-1 designed for clinical PET imaging. The development of an efficient and fully automated production sequence for [^{18}F] SynVesT-1, utilizing the Trasis AllinOne (AIO-36) module platform, has proven to be a significant advancement. With a decay-corrected radiochemical yield of approximately 21% and a radiochemical purity surpassing 99%, besides, the entire synthesis process was completed within a timeframe of 80 min (75 ± 3.1 min, $n=3$), saves 11 min compared to reported GMP automated synthesis procedures. The protocol ensures a high-quality pharmaceutical-grade solution of [^{18}F] SynVesT-1, deemed suitable for rigorous clinical studies. Notably, the Trasis AllinOne (AIO-36) module stands out as one of the most widely embraced fully automated synthesis platforms. Its adoption is anticipated to greatly contribute to the widespread synthesis and application of such probes, thereby advancing the field.

Abbreviations

SV2A	Synaptic vesicle glycoprotein 2 A
PET	Positron emission tomography
AIO	AllinOne
RCY	Radiochemical yields
RCP	Radiochemical purity
TOF	Time-of-flight
CT	Computed Tomography
MR	Magnetic Resonance
NED	Neuroendocrine
NETs	Neuroendocrine tumors
AD	Alzheimer's disease
PD	Parkinson's disease
UCB	Union Chimique Belge
GMP	Good manufacturing procedure
[^{18}F] FDG	Fluoro-2-deoxy-D-glucose
[^{18}F] F-DPA-714	[^{18}F] N, N-diethyl-2-(2-[4-(2-fluoroethoxy)phenyl]-5,7-dimethylpyrazolo[1,5- α]pyrimidine-3-yl)acetamide
[^{18}F] FAPI-74	[^{18}F] Fibroblast Activation Protein Inhibitor-74
[^{18}F] FES	16 α -18 F-17 β -fluoroestradiol
[^{18}F] FET	Fluoro-ethyl-tyrosine
[^{18}F] FMZ	Flumazenil
[^{18}F] DOPA	3,4-dihydroxyphenylalanine
[^{18}F] TSPO	Translocator protein
[^{68}Ga] DOTATATE	Tetraazacyclododecanetetraacetic acid-DPhe1-Tyr3-octreotate
QMA	Quaternary methyl ammonium
MeCN	Acetonitrile
HPLC	High-performance liquid chromatography
AcOH	Ethanoic acid
DMA	N, N-dimethylacetamide
EtOH	Ethanol
KOTf	Potassium triflate
DI	De-ionized
UV	Ultraviolet
FPV	Final product vial
QC	Quality control
ChP	Chinese Pharmacopoeia
GC	Gas Chromatography
CFU	Colony-Forming Unit
FT	Fluid thioglycolate
TSB	Tryptic soy broth
FID	Flame ionization detector
ICP-MS	Inductively coupled plasma mass spectrometry
ANOVA	Analysis of variance
SD	Standard deviation

ICH(Q3C) R8	International Council for Harmonisation, Impurities: Guideline for residual solvents, Revision 8
PDE	Permitted Daily Exposures
MIP	Maximum intensity projection

Acknowledgements

We thank Dr. Fang Xie and Dr. Jianfei Xiao from Huashan Hospital of Fudan University for providing precursors Me₃Sn-SDM-8 and standard sample, as well as offering advice on method details. We also appreciate Dr. Xuefei Li and Dr. Yangyang Xu for their valuable suggestions in establishing the methodology.

Author contributions

LJC, XCL and HQL performed radiochemical reactions; YG, RLL and XQW performed in-vitro studies; LJC, XNL and XSS performed QC studies; JFL helps build automated synthesis methods; WFZ and YPW carried out the experiment on PET/CT and PET/MR scanning; LJC wrote the main manuscript text; YJW and HQL read and commented on the paper; YB conceived and supervised the project; YPW and YG contributed significantly the data analysis; MYW made the conceptualization, funding acquisition, resources; All authors read and approved the final manuscript.

Funding

This work has been funded by the National Natural Science Foundation of China (Grant No. 82371934), the Science and Technology Project of Henan Province (Grant No. 242102311228), Henan Province Medical Science and Technology Research (Grant No. LHGJ20220059), and the Joint Fund of Henan Province Science and Technology R&D Program (Grant No. 225200810062).

Data availability

All data generated or analysed during this study are included in this published article.

Declarations

Ethics approval and consent to participate

The study was approved by the Research Ethics Committee of Henan Provincial people's hospital (2022, NO.163) and written informed consents were obtained from the subjects. All methods/procedures were performed in studies involving human participants in accordance with the ethical standards as laid down in the Declaration of Helsinki and its later amendments or comparable ethical standards.

Consent for publication

Written informed consent for publication was obtained from all participants.

Competing interests

The authors report no conflicts of interest.

Received: 25 May 2024 / Accepted: 9 July 2024

Published online: 10 September 2024

References

- Barnes C, Nair M, Aboagye EO, Archibald SJ, Allott L. A practical guide to automating fluorine-18 PET radiochemistry using commercially available cassette-based platforms. *Reaction Chem Eng.* 2022;7(11):2265–79. <https://doi.org/10.1039/d2re00219a>.
- Bastin C, Bahri MA, Meyer F, Manard M, Delhay E, Plenevaux A, Becker G, Seret A, Mella C, Giacomelli F, Degueldre C, Balteau E, Luxen A, Salmon E. In vivo imaging of synaptic loss in Alzheimer's disease with [¹⁸F]UCB-H positron emission tomography. *Eur J Nucl Med Mol Imaging.* 2020;47(2):390–402. <https://doi.org/10.1007/s00259-019-04461-x>.
- Bourgeron T. From the genetic architecture to synaptic plasticity in autism spectrum disorder. *Nat Reviews Neurosci (Vol. 2015;16(9):551–63.* <https://doi.org/10.1038/nrn3992>. Nature Publishing Group.
- Cai Z, Li S, Matuskey D, Nabulsi N, Huang Y. (2019). PET imaging of synaptic density: A new tool for investigation of neuropsychiatric diseases. In *Neuroscience Letters (Vol. 691, pp. 44–50)*. Elsevier Ireland Ltd. <https://doi.org/10.1016/j.neulet.2018.07.038>.
- Chen Z, Liao G, Wan N, He Z, Chen D, Tang Z, Long Z, Zou G, Peng L, Wan L, Wang C, Peng H, Shi Y, Tang Y, Li J, Li Y, Long T, Hou X, He L, Jiang H. Synaptic loss in Spinocerebellar Ataxia Type 3 revealed by SV2A Positron Emission Tomography. *Mov Disord.* 2023;38(6):978–89. <https://doi.org/10.1002/mds.29395>.
- Cybulska KA, Bloemers V, Perk LR, Laverman P. Optimised GMP-compliant production of [¹⁸F]DPA-714 on the Trasis AllinOne module. *EJNMMI Radiopharmacy Chem.* 2021a;6(1). <https://doi.org/10.1186/s41181-021-00133-0>.
- Cybulska KA, Bloemers V, Perk LR, Laverman P. Optimised GMP-compliant production of [¹⁸F]DPA-714 on the Trasis AllinOne module. *EJNMMI Radiopharmacy Chem.* 2021b;6(1). <https://doi.org/10.1186/s41181-021-00133-0>.
- Da Pieve C, Costa Braga M, Turton DR, Valla FA, Cakmak P, Plate K-H, Kramer-Marek G. New fully Automated Preparation of High Apparent Molar Activity ⁶⁸Ga-FAPI-46 on a Trasis AiO platform. *Molecules.* 2022;27(3). <https://doi.org/10.3390/molecules27030675>.
- Dahl K, Larsson S, Bonn P, Wallin A, Itsenko O, Schöll M. Good manufacturing procedure production of [¹⁸F]SynVesT-1, a radioligand for in vivo positron emission tomography imaging of synaptic vesicle glycoprotein 2A. *J Label Compd Radiopharm.* 2022;65(12):315–22. <https://doi.org/10.1002/jlcr.4002>.
- Delva A, Van Weehaeghe D, Koole M, Van Laere K, Vandenberghe W. Loss of Presynaptic Terminal Integrity in the Substantia Nigra in Early Parkinson's Disease. *Mov Disord.* 2020;35(11):1977–86. <https://doi.org/10.1002/mds.28216>.
- Estrada S, Lubberink M, Thibblin A, Sprycha M, Buchanan T, Mestdagh N, Kenda B, Mercier J, Provins L, Gillard M, Tytgat D, Antoni G. [¹¹C]UCB-A, a novel PET tracer for synaptic vesicle protein 2A. *Nucl Med Biol.* 2016;43(6):325–32. <https://doi.org/10.1016/j.nucmedbio.2016.03.004>.

- Gendron T, Destro G, Straathof NJW, Sap JBI, Guibbal F, Vriamont C, Caygill C, Attack JR, Watkins AJ, Marshall C, Hueting R, Warnier C, Gouverneur V, Tredwell M. Multi-patient dose synthesis of [¹⁸F] Flumazenil via a copper-mediated ¹⁸F-fluorination. *EJNMMI Radiopharmacy Chem.* 2022;7(1). <https://doi.org/10.1186/s41181-022-00158-z>.
- Georgantzis K, Tsolakis AV, Jakobson Å, Christofferson R, Janson ET, Grimelius L. Synaptic vesicle protein 2 and vesicular monoamine transporter 1 and 2 are expressed in Neuroblastoma. *Endocr Pathol.* 2019;30(3):173–9. <https://doi.org/10.1007/s12022-019-09584-3>.
- Guan B, Zhou N, Wu CY, Li S, Chen YA, Debnath S, Hofstad M, Ma S, Raj GV, He D, Hsieh JT, Huang Y, Hao G, Sun X. Validation of sv2a-targeted pet imaging for noninvasive assessment of neuroendocrine differentiation in prostate cancer. *Int J Mol Sci.* 2021;22(23). <https://doi.org/10.3390/ijms222313085>.
- Holmes SE, Scheinost D, Finnema SJ, Naganawa M, Davis MT, DellaGioia N, Nabulsi N, Matuskey D, Angarita GA, Pietrzak RH, Duman RS, Sanacora G, Krystal JH, Carson RE, Esterlis I. Lower synaptic density is associated with depression severity and network alterations. *Nat Commun.* 2019;10(1). <https://doi.org/10.1038/s41467-019-09562-7>.
- Huang Z, Wu Y, Fu F, Meng N, Gu F, Wu Q, Hu Z. Parametric image generation with the uEXPLORER total-body PET/CT system through deep learning. *Eur J Nucl Med Mol Imaging.* 2022;49(8):2482–92. <https://doi.org/10.1007/s00259-022-05731-x>.
- Jakobsen AM, Ahlman H, Wängberg B, Kölby L, Bengtsson M, Nilsson O. Expression of synaptic vesicle protein 2 (SV2) in neuroendocrine tumours of the gastrointestinal tract and pancreas. *J Pathol.* 2002;196(1):44–50. <https://doi.org/10.1002/path.1002>.
- Jamjoom AAB, Rhodes J, Andrews PJD, Grant SGN. The synapse in traumatic brain injury. *Brain.* Volume 144. Oxford University Press; 2021. pp. 18–31. <https://doi.org/10.1093/brain/awaa321>.
- Li S, Cai Z, Wu X, Holden D, Pracitto R, Kapinos M, Gao H, Labaree D, Nabulsi N, Carson RE, Huang Y. Synthesis and in vivo evaluation of a novel PET Radiotracer for imaging of synaptic vesicle glycoprotein 2A (SV2A) in Nonhuman Primates. *ACS Chem Neurosci.* 2019;10(3):1544–54. <https://doi.org/10.1021/acscchemneuro.8b00526>.
- Li S, Naganawa M, Pracitto R, Najafzadeh S, Holden D, Henry S, et al. Assessment of test-retest reproducibility of [¹⁸F]SynVesT-1, a novel radiotracer for PET imaging of synaptic vesicle glycoprotein 2A. *Eur J Nucl Med Mol Imaging.* 2021;48:1327–38. <https://doi.org/10.1007/s00259-020-05149-3>.
- Martin SL, Uribe C, Strafella AP. PET imaging of synaptic density in parkinsonian disorders. *Journal of Neuroscience Research.* John Wiley and Sons Inc; 2023. <https://doi.org/10.1002/jnr.25253>.
- Mecca AP, Chen MK, O'Dell RS, Naganawa M, Toyonaga T, Godek TA, Harris JE, Bartlett HH, Zhao W, Nabulsi NB, Wyk BCV, Varma P, Arnsten AFT, Huang Y, Carson RE, van Dyck CH. In vivo measurement of widespread synaptic loss in Alzheimer's disease with SV2A PET. *Alzheimer's Dement.* 2020;16(7):974–82. <https://doi.org/10.1002/alz.12097>.
- Mecca AP, O'Dell RS, Sharp ES, Banks ER, Bartlett HH, Zhao W, Lipior S, Diepenbrock NG, Chen MK, Naganawa M, Toyonaga T, Nabulsi NB, Wyk V, Arnsten BC, Huang AFT, Carson Y, R. E., van Dyck CH. Synaptic density and cognitive performance in Alzheimer's disease: a PET imaging study with [¹¹C]UCB-J. *Alzheimer's Dement.* 2022;18(12):2527–36. <https://doi.org/10.1002/alz.12582>.
- Michiels L, Mertens N, Thijs L, Radwan A, Sunaert S, Vandenbulcke M, Verheyden G, Koole M, Van Laere K, Lemmens R. Changes in synaptic density in the subacute phase after ischemic stroke: a ¹¹C-UCB-J PET/MR study. *J Cereb Blood Flow Metab.* 2022;42(2):303–14. <https://doi.org/10.1177/0271678X211047759>.
- Michiels L, Thijs L, Mertens N, Coremans M, Vandenbulcke M, Verheyden G, Koole M, Van Laere K, Lemmens R. Longitudinal synaptic density PET with ¹¹C-UCB-J 6 months after ischemic stroke. *Ann Neurol.* 2023;93(5):911–21. <https://doi.org/10.1002/ana.26593>.
- Otabashi M, Vergote T, Desfours C. Efficient commercial scale ¹⁸F-FES production on AllinOne (Trasis). *J Nucl Med.* 2017a;58(supplement 1):878. https://jnm.snmjournals.org/content/58/supplement_1/878.
- Otabashi M, Vergote T, Desfours C. High yield ¹⁸F-FET production on AllinOne (Trasis) at commercial scale. *J Nucl Med.* 2017b;58(supplement 1):879. https://jnm.snmjournals.org/content/58/supplement_1/879.
- Portela-Gomes M, Lukinius G, A., Grimelius L. (2000). Synaptic vesicle protein 2, a new neuroendocrine cell marker. *In Am J Pathol* (157).
- Samantha Rossano T, Toyonaga J, Bini N, Nabulsi J, Ropchan Z, Cai Y, Huang RE, Carson. Feasibility of imaging synaptic density in the human spinal cord using [¹¹C] UCB-J PET. *EJNMMI Phys.* 2022;9:32. <https://doi.org/10.1186/s40658-022-00464-0>.
- Serdons K, Alfons V, Guy B. The presence of ethanol in radiopharmaceutical injections. *J Nucl Med.* 2008;4912:2071–2071. <https://doi.org/10.2967/jnumed.108.057026>.
- Tang Y, Yu J, Zhou M, Li J, Long T, Li Y, Feng L, Chen D, Yang Z, Huang Y, Hu S. Cortical abnormalities of synaptic vesicle protein 2A in focal cortical dysplasia type II identified in vivo with ¹⁸F-SynVesT-1 positron emission tomography imaging. *Eur J Nucl Med Mol Imaging.* 2022;49(10):3482–91. <https://doi.org/10.1007/s00259-021-05665-w>.
- Wiedenmann B, Franke WW, Kuhn C, Moll R, Gould VE. (1986). Synaptophysin: A marker protein for neuroendocrine cells and neoplasms (synaptic vesicles/neurosecretory granules/pancreatic islets/carcinoids/tumor diagnosis). *In Medical Sciences* (Vol. 83). <https://www.pnas.org>.

Publisher's Note

Springer Nature remains neutral with regard to jurisdictional claims in published maps and institutional affiliations.